

ORIGINAL ARTICLE

Targeting HSP90 and monoclonal protein trafficking modulates the unfolded protein response, chaperone regulation and apoptosis in myeloma cells

EJ Born¹, SV Hartman² and SA Holstein¹

Multiple myeloma is characterized by the production of substantial quantities of monoclonal protein. We have previously demonstrated that select inhibitors of the isoprenoid biosynthetic pathway (IBP) induce apoptosis of myeloma cells via inhibition of Rab geranylgeranylation, leading to disruption of monoclonal protein trafficking and induction of the unfolded protein response (UPR) pathway. Heat-shock protein 90 (HSP90) inhibitors disrupt protein folding and are currently under clinical investigation in myeloma. The effects of combining IBP and HSP90 inhibitors on cell death, monoclonal protein trafficking, the UPR and chaperone regulation were investigated in monoclonal protein-producing cells. An enhanced induction of cell death was observed following treatment with IBP and HSP90 inhibitors, which occurred through both ER stress and non-ER stress pathways. The HSP90 inhibitor 17-AAG abrogated the effects of the IBP inhibitors on intracellular monoclonal protein levels and localization as well as induction of the UPR in myeloma cells. Disparate effects on chaperone expression were observed in myeloma vs amyloid light chain cells. Here we demonstrate that the novel strategy of targeting MP trafficking in concert with HSP90 enhances myeloma cell death via a complex modulation of ER stress, UPR, and cell death pathways.

Blood Cancer Journal (2013) 3, e167; doi:10.1038/bcj.2013.64; published online 6 December 2013

Keywords: HSP90; unfolded protein response pathway; multiple myeloma; Rab; amyloid

INTRODUCTION

Multiple myeloma is a plasma cell dyscrasia characterized by the production of monoclonal protein (MP). Although the last decade has seen to the introduction of new therapeutic agents that have resulted in improvements in overall survival, patients still develop refractory disease, and there remains a need for the development of novel therapeutic strategies. Recently there has been considerable interest in the use of heat-shock protein 90 (HSP90) inhibitors in myeloma. HSP90 is a key molecular chaperone protein for over a hundred different client proteins, many of which are critical for cell survival and proliferation. Inhibitors of HSP90 such as geldanamycin and its analog 17-AAG have been demonstrated to result in disruption of normal protein folding and induction of cell death.¹ There has been particular interest in the cytotoxic activities of HSP90 inhibitors in myeloma.^{2–4} Synergistic activity between HSP90 inhibitors and proteasome inhibitors have been observed.^{2,4,5} Early-stage clinical trials involving the combination of bortezomib and 17-AAG have been conducted and have demonstrated evidence of response in bortezomib-naive, pre-treated and even refractory myeloma patients.⁵

A marked expansion of the endoplasmic reticulum (ER) occurs during the differentiation from B cell to plasma cell, thus providing the necessary machinery for efficient production of antibodies.⁷ This differentiation is associated with upregulation of the pro-survival components of the unfolded protein response pathway (UPR). The three transducers of the UPR are inositol-requiring kinase 1 (Ire1), activating transcription factor-6 (ATF6), and protein kinase RNA-like ER kinase (PERK).⁸ Activation of Ire1 and ATF6 leads to transcription of multiple UPR target genes, including

protein chaperones and folding enzymes.⁹ PERK activation results in the phosphorylation of eIF2 α , inducing a decrease in global protein synthesis.¹⁰ Induction of the UPR by ER stress initially serves as a protective mechanism by increasing the cell capacity for protein folding, however, if the stress is too severe or prolonged, then UPR activation can result in apoptosis. UPR-mediated apoptosis involves induction of GADD153/CHOP and cleavage and activation of caspases.¹¹ GADD153 is induced via both the PERK and ATF6 UPR pathways.^{12,13} Caspase-4 (caspase-12 in the mouse) is believed to serve as the initiator caspase in ER stress-induced apoptosis, leading to the cleavage of caspase-9 and, in turn, the activation of caspase-3.^{14,15} The caspase-12/caspase-4-mediated apoptotic pathway has been postulated to be distinct from the classic intrinsic or extrinsic apoptotic pathways.¹⁶ The activation of caspase-2 has been associated with ER stress-induced apoptosis in myeloma cells following treatment with bortezomib.¹⁷ Myeloma cells, compared with non-secretory cells, have a lower threshold for induction of the pro-apoptotic components of the UPR as a consequence of near-maximal expression of the protective UPR elements.¹⁸ We have previously demonstrated that disruption of MP trafficking via agents that interfere with Rab geranylgeranylation leads to accumulation of MP in the ER, induction of the UPR and apoptosis in myeloma cells.¹⁹

We therefore hypothesized that the approach of combining agents, which inhibit HSP90 and disrupt MP trafficking, would lead to enhanced derailment of MP homeostasis, which in turn would lead to enhanced myeloma cell death. 17-AAG and lovastatin were chosen as representative inhibitors of HSP90 and Rab

¹Department of Internal Medicine, University of Iowa, Iowa City, IA, USA and ²Integrated DNA Technologies, Coralville, IA, USA. Correspondence: Dr SA Holstein, Department of Internal Medicine, 200 Hawkins Dr, C32 GH, Iowa City, IA 52242, USA.

E-mail: sarah-holstein@uiowa.edu

Received 24 September 2013; accepted 6 November 2013

geranylgeranylation, respectively. Here we demonstrate that this novel strategy is characterized by a complex interaction involving regulation of chaperone expression, MP trafficking, activation of the UPR and induction of apoptotic pathways.

MATERIAL AND METHODS

Reagents

Lovastatin, brefeldin A and 4-phenylbutyric acid were obtained from Sigma (St Louis, MO, USA). 17-AAG, FTI-277 and GGTI-2133 were purchased from Santa Cruz Biotechnology (Santa Cruz, CA, USA). Bortezomib was obtained from Millenium Pharmaceuticals. Digeranyl bisphosphonate (DGBP)²⁰ and 3-PEHPC²¹ were kindly provided by Professor David Wiemer, Department of Chemistry, University of Iowa. Anti- β -tubulin, anti-calnexin, anti-PARP, anti-HSP70, anti-HSP90 α/β and anti-goat IgG horseradish peroxidase (HRP) antibodies were purchased from Santa Cruz Biotechnology. Anti-eIF2 α , anti-phospho-eIF2 α , anti-cleaved caspase-8, anti-cleaved caspase-9 and anti-cleaved caspase-3 antibodies were obtained from Cell Signaling Technology (Danvers, MA, USA). Anti-mouse and anti-rabbit HRP-linked antibodies were obtained from Amersham (GE Healthcare, Pittsburg, PA, USA). Z-VDVAD-FMK, Z-YVAD-FMK and Z-VAD-FMK were purchased from R&D Systems. (Minneapolis, MN, USA).

Cell culture

Human myeloma (RPMI-8226, U266, H929, MM.1S, MC/CAR) and the RL lymphoblastoid cell lines were purchased from American Type Culture Collection (ATCC) (Manassas, VA, USA). Cells were grown in media (per ATCC specifications) supplemented with heat-inactivated fetal calf serum (FCS), glutamine and penicillin-streptomycin at 37 °C and 5% CO₂. ALMC-2 cells were obtained from Dr Diane Jelinek, Mayo Clinic (Rochester, MN, USA) and were grown in Iscove-modified Dubelco medium supplemented with FCS, glutamine, penicillin-streptomycin, IL-6 and IGF-1.²²

MTT assay

Cells were seeded (5×10^4 cells/150 μ l per well) in 96-well flat-bottom plates and incubated with drugs for 48 h. The MTT assay was performed as previously described.²³ The absorbance for control cells treated with solvent only was defined as an MTT activity of 100%.

Monoclonal protein quantitation

Cells were incubated in the presence or absence of drugs for specified periods of time. The cells were lysed in RIPA buffer (0.15 M NaCl, 1% sodium deoxycholate, 0.1% SDS, 1% Triton (v/v) X-100, 0.05 M Tris-HCl) containing protease and phosphatase inhibitors. Protein content was determined using the bicinchoninic acid (BCA) method. Human lambda light chain kit (Bethyl Laboratories, Montgomery, TX, USA) was used to quantify intracellular and secreted monoclonal protein levels.

Immunoblotting

Following incubation with drugs, cells were collected, washed with PBS, and lysed in RIPA buffer as described above. Protein content was determined using the BCA method. Equivalent amounts of cell lysate were resolved by SDS-PAGE, transferred to polyvinylidene difluoride membrane, probed with the appropriate primary antibodies and detected using HRP-linked secondary antibodies and Amersham Pharmacia Biotech ECL western blotting reagents per manufacturer's protocols. For β -tubulin, calnexin, PARP, HSP90 and HSP70, the membranes were probed with the primary antibody for 1 h at 37 °C. For eIF2 α , phospho-eIF2 α , cleaved caspase-8, IRE1 α , cleaved caspase-9 and cleaved caspase-3, membranes were incubated with the primary antibody overnight at 4 °C (Supplementary Table 1).

Quantitative real-time PCR

Cells were grown in the absence or presence of drugs for 24 or 48 h. Each condition was performed in triplicate. RNA was isolated using an RNeasy kit (Qiagen, Germantown, MD, USA), and a BioRad cDNA synthesis kit was used to prepare cDNA. Primers for PERK, GADD153, ATF6, IRE1, HSP70, HSC70, GRP78, GRP94 and β -actin (Supplementary Table 2) were designed using PrimerQuest. Real-time PCR was performed on an Applied Biosystems (Life Technologies, Grand Island, NY, USA) Model 7900HT using an Applied Biosystems reaction kit with SYBR green. Data were analyzed using ABI SDS 2.3 software (Qiagen) and normalized to β -actin

RNA. Quantities were determined using the relative standard curve method. Each sample was run in triplicate.

siRNA transfection

HSP90 α/β siRNA and scrambled control siRNA were purchased from Santa Cruz Biotechnology. Nucleofection of RPMI-8226 cells (2×10^6) was carried out using an Amaxa nucleofactor II with solution V, program G16. Twenty-four hours after nucleofection, lovastatin was added, and cells were incubated for an additional 48 h.

Immunofluorescence microscopy studies

Cells were grown on poly-L-lysine-coated coverslips. Following incubation with the drugs, cells were fixed with 4% paraformaldehyde and then permeabilized in 0.1% Triton X-100. Staining for lambda light chain and PDI was performed as previously described.¹⁹ The coverslips were mounted in Vecta-Shield with DAPI. Microscopy was performed using a Zeiss LSM 710 confocal microscope with a $\times 60$ objective at the University of Iowa Central Microscopy Research Facilities. Images were processed using ImageJ software (National Institutes of Health, Bethesda, MD, USA). The merged images represent merging of the lambda, PDI and DAPI images via ImageJ software.

Statistics

Two-tailed *t*-testing was used to calculate statistical significance. An α of 0.05 was set as the level of significance. Isobologram analysis was used to evaluate the data from the MTT assays via CalcuSyn software (Biosoft, Great Shelford, Cambridge, UK). The software analyzes drug interactions based on the method of Chou and Talalay.²⁴

RESULTS

The effects of combining 17-AAG, an HSP90 inhibitor, with IBP inhibitors were investigated via a series of MTT assays. Lovastatin, a HMG-CoA reductase inhibitor, depletes cells of all isoprenoids downstream of mevalonate, including geranylgeranyl pyrophosphate (GGPP) while 3-PEHPC is a direct inhibitor of GGTase II. It was hypothesized that these agents, which disrupt MP trafficking,¹⁹ would enhance cytotoxicity when combined with 17-AAG. Four human myeloma cell lines (RPMI-8226, U266, H929, MM.1S), a human light chain amyloid cell line (ALMC-2), an EBV-transformed B-lymphoblastoid cell line (MC/CAR) and a human lymphoblastoid cell line (RL) were evaluated. These lines differ with respect to MP production/secretion, with the MC/CAR and RL lines producing and secreting very low levels (Supplementary Table 3). Cells were treated with the agents either concurrently for 48 h or were pre-treated with the IBP inhibitor for 24 h before the addition of 17-AAG. Isobologram analysis was performed to determine the nature of the interaction. This analysis revealed that the combination of these agents yielded synergistic effects in the RPMI-8226 cells and additive or synergistic effects in the U266 and MM.1S cells (Table 1). Studies performed in the H929 cells did not reveal a consistent pattern of interaction for concurrent incubations but did show additive effects following IBP pre-treatment. The ALMC-2 cells are relatively resistant to 3-PEHPC, and therefore formal isobologram analysis could not be performed. In the MC/CAR and RL cells, lovastatin and 17-AAG induced additive cytotoxic effects, whereas 3-PEHPC and 17-AAG induced antagonistic effects. Overall, these studies suggest that those cells that produce and secrete MP most efficiently are the most sensitive with respect to the cytotoxic effects of combining IBP and HSP90 inhibitors.

To determine whether the enhanced cytotoxic effects observed in the MTT studies correlated with enhanced induction of apoptosis in myeloma cells, immunoblot analysis was used to assess for cleavage of PARP, calnexin, caspase-8, caspase-3 and caspase-9. As shown in Figure 1a, treatment of RPMI-8226 or H929 cells with 17-AAG results in a concentration-dependent induction of PARP, calnexin, caspase-3, caspase-8 and caspase-9 cleavage. The addition of lovastatin further enhances these effects.

Table 1. Summary of interactions between IBP inhibitors and 17-AAG in myeloma cells

| IBP inhibitor | Cell line | | | | | | |
|-------------------------------|------------|------------|------------|------------|--------------------------|------------|------------|
| | RPMI-8226 | U266 | MM.1S | H929 | ALMC-2 | MC/CAR | RL |
| <i>Concurrent with 17-AAG</i> | | | | | | | |
| Lov | Syn (0.56) | Add (1.00) | Add (0.95) | Ant (1.32) | Add (0.88) | Add (0.84) | Add (1.12) |
| 3-PEHPC | Syn (0.66) | Add (0.87) | Add (0.93) | Syn (0.75) | Insensitive ^a | Ant (1.5) | Ant (1.29) |
| <i>Pre-treatment</i> | | | | | | | |
| Lov | Syn (0.31) | Syn (0.58) | Add (1.19) | Add (0.91) | Add (0.83) | Add (1.17) | Add (1.09) |
| 3-PEHPC | Syn (0.67) | Syn (0.67) | Add (0.95) | Add (0.82) | Insensitive | Ant (1.59) | Ant (1.85) |

Cells were incubated in the presence of an IBP inhibitor (1–25 μM lovastatin (*Lov*) or 0.2–5 mM 3-PEHPC) and/or 17-AAG (0.1–2.5 μM) for either 48 h concurrently or 24 h pre-treatment with IBP inhibitor followed by a 24-h concurrent treatment with 17-AAG. MTT cytotoxicity assays were performed. Isobologram analysis was used to determine the combination indices (CI) for each drug combination for ED₃₀ (CI shown in parenthesis). An interaction was determined to be synergistic (*Syn*) if the CI was <0.8, antagonistic (*Ant*) if the CI was >1.2 and additive (*Add*) for CI between 0.8 and 1.2. The CIs are representative of 2–3 independent experiments. ^aAt tested concentrations, 3-PEHPC induced less than a 10% decrease in MTT activity in ALMC-2 cells, and therefore isobologram analysis was not performed.

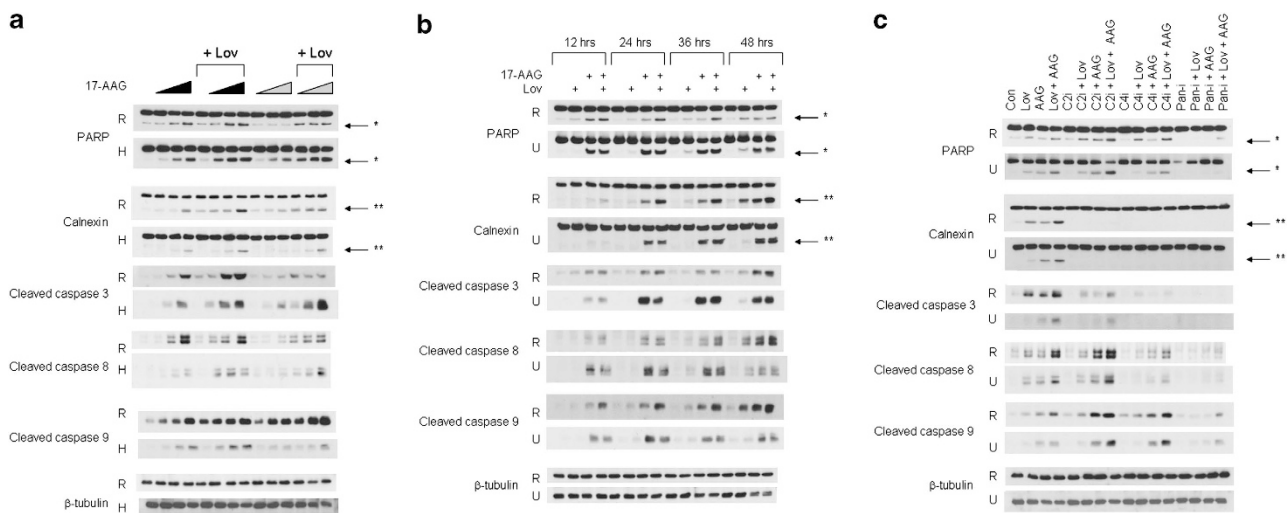


Figure 1. Simultaneous inhibition of HSP90 and the IBP results in the induction of apoptosis of myeloma cells. Immunoblots depicting PARP, calnexin, cleaved caspase 3, cleaved caspase 8, cleaved caspase 9 and β -tubulin are shown. * denotes the PARP cleavage product while ** denotes the calnexin cleavage product. β -Tubulin is used as a loading control. Data are representative of at least three independent experiments. (a) RPMI-8226 (R) and H929 (H) cells were incubated with lovastatin (*Lov*, 10 μM for RPMI-8226 and 2.5 μM for H929) and/or varying concentrations of 17-AAG (AAG) for a total of 48 h. The wedges indicate increasing concentrations of 17-AAG (0.1, 0.5, 1 μM for RPMI-8226 cells and 0.05, 0.1, 0.25 μM for H929 cells). The black wedges indicate that 17-AAG was added at the start of the 48-h incubation, whereas the gray wedges indicate that 17-AAG was added after 24 h. (b) RPMI-8226 (R) and U266 (U) cells were cultured for 12–48 h in the presence or absence of lovastatin (10 μM) and/or 17-AAG (0.5 μM). (c) Effects of caspase inhibitors on 17-AAG- and lovastatin-induced apoptosis. RPMI-8226 and U266 cells were incubated for 48 h in the presence or absence of 17-AAG (0.5 μM), lovastatin (10 μM), caspase-2 inhibitor (50 μM VD-VAD, *C2i*), caspase-4 inhibitor (50 μM Y-VAD, *C4i*) or pan-caspase inhibitor (50 μM VAD, *Pan-i*).

These effects were observed when lovastatin and 17-AAG were administered concurrently for 48 h as well as when 17-AAG was added following 24 h of lovastatin pre-treatment. Similar effects were observed in RPMI-8226 cells treated with 17-AAG and with either digeranyl bisphosphonate or 3-PEHPC (data not shown). Annexin V/propidium iodide (PI) flow cytometry studies confirmed enhanced induction of apoptosis in RPMI-8226 cells (Supplementary Figure 1). Time course experiments performed in RPMI-8226 and U266 cells demonstrated a time-dependent increase in apoptotic markers and that the cleavage of PARP and caspases 3, 8 and 9 precedes calnexin cleavage (Figure 1b). While the effects of 17-AAG on these apoptotic markers occurred early in the time course (cleavage seen at 12 h), the maximal effect of lovastatin was not observed until 48 h.

Both caspase-2 and caspase-4 have been reported to have roles in ER stress-mediated apoptosis.^{17,25,26} Studies were performed in which RPMI-8226 or U266 cells were treated with 17-AAG and/or lovastatin in combination with specific caspase-2, caspase-4 or pan-caspase inhibitors (Figure 1c). As expected, the pan-caspase inhibitor prevented 17-AAG- and/or lovastatin-induced PARP and calnexin cleavage as well as cleavage of caspases 3, 8 and 9 in all tested cell lines. The caspase-2 and caspase-4 inhibitors completely prevented the cleavage of calnexin and partially suppressed caspase-3 cleavage but did not prevent PARP or caspase-9 cleavage. In contrast, both the caspase-2 and caspase-4 specific inhibitors partially prevented PARP, caspase 3 and caspase 9 cleavage in the ALMC-2 cells while completely preventing calnexin cleavage (Supplementary Figure 2). While U266 cells appear to

lack expression of caspase-4,²⁷ RPMI-8226 and ALMC-2 cells do express caspase-4 (Supplementary Figure 3). That the caspase 4 inhibitor displayed some activity in the U266 cells suggests either minimal expression of caspase-4 or lack of specificity of the inhibitor. Overall, these studies demonstrate that combination therapy results in induction of apoptosis of myeloma cells via multiple pathways, including ER stress, intrinsic and extrinsic pathways.

We have previously demonstrated that select IBP inhibitors disrupt MP trafficking, resulting in an accumulation of intracellular MP,¹⁹ and others have reported the presence of inclusion bodies containing MP following HSP90 inhibitor treatment.²⁸ We therefore evaluated the effects of combining these agents on MP levels. Addition of 17-AAG to an IBP inhibitor (lovastatin, digeranyl bisphosphonate, or 3-PEHPC) in RPMI-8226 cells partially decreased the IBP inhibitor-induced accumulation of intracellular MP levels (Figure 2a). Immunoblot analysis utilizing anti-lambda light chain antibodies confirmed the abrogation of lovastatin's

effects by 17-AAG on intracellular levels in RPMI-8226 cells (data not shown). The effect of 17-AAG on lovastatin-induced accumulation of intracellular lambda light chain was observed across multiple time points (Figure 2b). Similar results were observed in U266 cells treated with lovastatin and 17-AAG (Supplementary Figure 4). These observed effects were not a result of either increased light chain secretion or effects on light chain mRNA levels. The addition of 17-AAG to lovastatin enhanced the observed decrease in secreted light chain induced by lovastatin in RPMI-8226 cells (Supplementary Figure 5). Neither lovastatin nor 17-AAG induced changes in lambda light chain mRNA levels in RPMI-8226 or U266 cells (Supplementary Figure 6). In contrast to the myeloma lines, the combination of lovastatin and 17-AAG led to enhanced accumulation of intracellular MP levels in the ALMC-2 cells compared with either agent alone (Figure 2c).

As a non-pharmacological approach with which to inhibit HSP90, RPMI-8226 cells were transfected with HSP90 α/β siRNA and incubated in the absence or presence of lovastatin.

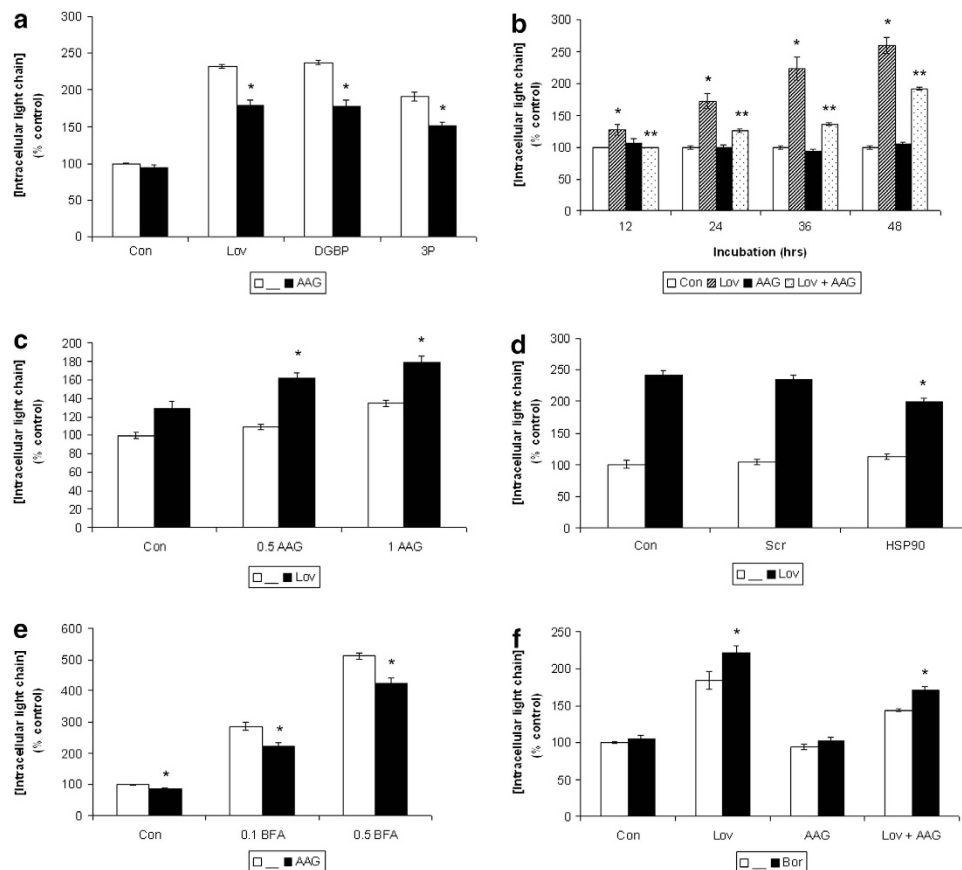


Figure 2. Effects of targeting HSP90 on monoclonal protein trafficking. Intracellular lambda light chain levels were measured via ELISA. Data are expressed as percentage of control (mean \pm s.d., $n = 3$) and are representative of at least two independent experiments. (a) RPMI-8226 cells were incubated for 48 h in the presence or absence of 0.5 μ M 17-AAG (AAG) in combination with either 10 μ M lovastatin (Lov), 10 μ M digeranyl bisphosphonate (DGBP) or 5 mM 3-PEHPC (3P). The * denotes $P < 0.05$ per unpaired two-tailed t -test and compares treatments with and without 17-AAG. (b) RPMI-8226 cells were incubated for 12–48 h in the presence or absence of 10 μ M lovastatin (Lov) and/or 0.5 μ M 17-AAG (AAG). The * denotes $P < 0.05$ per unpaired two-tailed t -test and compares lovastatin-treated cells to control cells. The ** denotes $P < 0.05$ per unpaired two-tailed t -test and compares lovastatin + 17-AAG-treated cells with lovastatin alone. (c) ALMC-2 cells were incubated for 48 h in the presence or absence of 10 μ M lovastatin (Lov) in combination with 0.5 or 1 μ M 17-AAG (AAG). The * denotes $P < 0.05$ per unpaired two-tailed t -test and compares treatments with and without 17-AAG. (d) RPMI-8226 cells were nucleofected with HSP90 α/β siRNA (HSP90) or scrambled siRNA (Scr). After 24 h, cells were treated in the presence or absence of 10 μ M lovastatin (Lov) for an additional 48 h. The * denotes $P < 0.05$ per unpaired two-tailed t -test and compares the transfected cells to the untransfected cells (control or lovastatin). (e) RPMI-8226 cells were incubated for 24 h in the presence or absence of 0.5 μ M 17-AAG (AAG) and brefeldin A (BFA, 0.1 or 0.5 μ M). The * denotes $P < 0.05$ per unpaired two-tailed t -test and compares treatments with and without 17-AAG. (f) Addition of a proteasome inhibitor augments the effects of lovastatin and 17-AAG. RPMI-8226 cells were incubated for 48 h in the presence or absence of 10 μ M lovastatin (Lov), 0.5 μ M 17-AAG (AAG) and 2.5 nM bortezomib (Bor). The * denotes $P < 0.05$ per unpaired two-tailed t -test and compares treatments with and without bortezomib.

Transfection of cells with the HSP90 siRNA resulted in a decrease in HSP90 and an increase in HSP70 protein levels (Supplementary Figure 7). Whereas transfection of scrambled siRNA did not significantly alter intracellular light chain levels, transfection of HSP90 siRNA did partially abrogate the lovastatin-induced increase in light chain level (Figure 2d).

Brefeldin A (BFA), a known inhibitor of ER to Golgi transport,²⁹ was used as an alternative means of disrupting MP trafficking. Treatment of RPMI-8226 cells with BFA induced a marked intracellular accumulation of lambda light chain (Figure 2e). Similar to the studies with the IBP inhibitors, co-incubation with 17-AAG partially abrogated this effect.

One possible mechanism underlying the observed decrease in intracellular light chain level in myeloma cells is enhanced proteasomal degradation. To explore this hypothesis, cells were incubated in the presence or absence of the proteasome inhibitor bortezomib. Whereas bortezomib did not significantly alter levels of intracellular light chain in RPMI-8226 cells treated with 17-AAG, it did lead to a mild increase in intracellular protein when combined with either lovastatin or lovastatin plus 17-AAG (Figure 2f). Similar effects were observed in U266 cells (data not shown).

To determine whether HSP90 inhibition alters the effects of lovastatin-induced changes in intracellular lambda light chain localization, indirect immunofluorescent microscopy studies were performed in RPMI-8226 cells. As shown in Figure 3, and consistent with our previous studies,¹⁹ under control conditions the staining pattern for lambda light chain is primarily peri-nuclear as well as a more diffuse vesicular-like pattern through-out the cytoplasm that does not co-localize with a marker for the ER (PDI).

Following treatment with lovastatin, there is an accumulation of lambda light chain primarily within the ER, as evidenced by co-localization with PDI. In contrast, treatment with 17-AAG diminished the cytoplasmic staining of lambda light chain with the majority of the staining localized to the peri-nuclear region. For cells treated with both agents, the localization pattern of lambda light chain appeared less homogenous with respect to ER localization than that observed with lovastatin alone. Three-dimensional rendering of these images supported these findings (Supplementary Figure 8).

To explore the effects of targeting HSP90 and Rab prenylation on the UPR, myeloma and amyloid cells were co-incubated with 17-AAG and lovastatin. Treatment with lovastatin induces expression of the three transducers of the UPR (PERK, IRE1, and ATF6) as well as GADD153 (Figure 4a). Although lovastatin globally diminishes protein prenylation, the observed effects on the UPR can be attributed to disruption of Rab geranylgeranylation as a specific GGTase II inhibitor, but not FTase or GGTase I inhibitors, induce the UPR in a similar manner (Supplementary Figure 9). In the three tested myeloma lines, the addition of 17-AAG suppressed the lovastatin-induced upregulation of the UPR mediators (Figure 4a). In contrast, a mixed picture was observed in the ALMC-2 cells, where the drug combination yielded an increase in ATF6 and IRE1 levels. Immunoblot analysis confirmed these findings (Supplementary Figure 10).

Quantitative PCR studies demonstrated that BFA induces upregulation of all three transducers of the UPR (PERK, ATF6, IRE1) as well as GADD153 (Figure 4b) in RPMI-8226 cells. Co-incubation with 17-AAG partially prevented the BFA-induced upregulation of ATF6, IRE1 and GADD153 (Figure 4b). As another

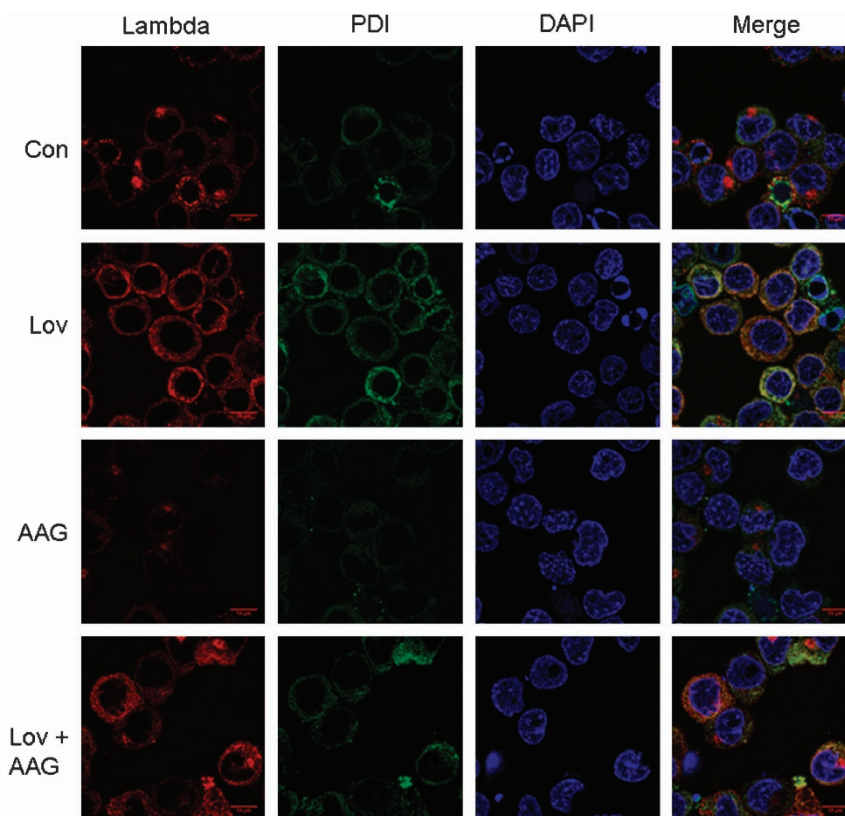


Figure 3. Changes in intracellular lambda light chain localization following drug treatment. RPMI-8226 cells were incubated in the absence or presence of 10 μ M lovastatin (*Lov*) and/or 0.5 μ M 17-AAG (*AAG*) for 24 h. Indirect immunofluorescence microscopy was performed as described in the Materials and Methods section using antibodies directed against lambda light chain and PDI. DAPI was used for nuclear staining. The merged images represent merging of the lambda, PDI and DAPI images via ImageJ software.

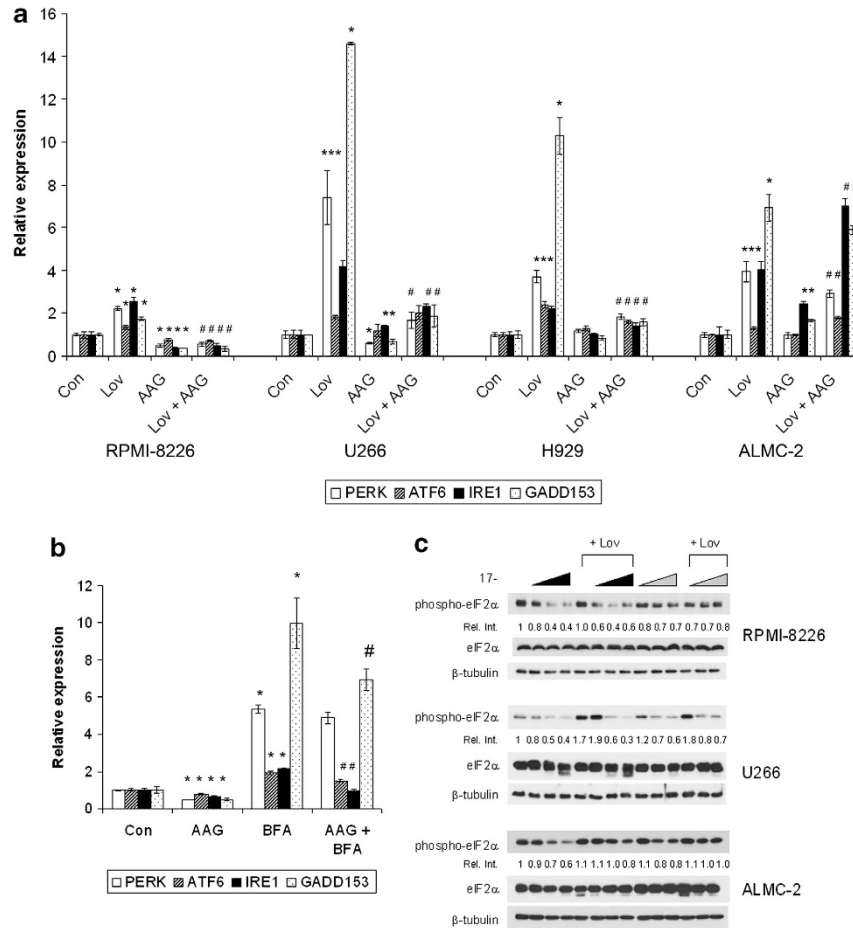


Figure 4. Effects of HSP90 and IBP inhibition on components of the UPR. **(a)** RPMI-8226, U266, H929 and ALMC-2 cells were incubated for 48 h in the presence or absence of lovastatin (*Lov*) and/or 17-AAG (AAG). For the RPMI-8226, U266 and ALMC-2 cells, 10 μM lovastatin and 0.5 μM 17-AAG were used, whereas for the H929 cells, 2.5 μM lovastatin and 0.25 μM 17-AAG were used. Real-time PCR was performed using primers for PERK, ATF6, IRE1 and GADD153. Data were normalized to β -actin levels and are expressed as relative to control untreated cells (mean \pm s.d., $n = 3$). Data are representative of two independent experiments. The * denotes $P < 0.05$ per unpaired two-tailed t -test and compares treated cells with control cells. The # denotes $P < 0.05$ for the combination of lovastatin + 17-AAG compared with lovastatin alone. **(b)** Real-time PCR was performed using primers for PERK, ATF6, IRE1 and GADD153 following incubation of RPMI-8226 cells with 0.5 μM 17-AAG (AAG) and/or 0.5 μM brefeldin A (BFA) for 24 h. Data are normalized to β -actin levels and are expressed as relative to control untreated cells (mean \pm s.d., $n = 3$). Data are representative of two independent experiments. The * denotes $P < 0.05$ per unpaired two-tailed t -test and compares treated cells to control cells. The # denotes $P < 0.05$ for the combination of 17-AAG and BFA compared with BFA alone. **(c)** Immunoblots depicting phosphorylated eIF2 α (*phospho-eIF2 α*), eIF2 α and β -tubulin (loading control) from RPMI-8226, U266 or ALMC-2 cells treated with 10 μM lovastatin (*Lov*) and/or 17-AAG (AAG). The wedges indicate increasing concentrations of 17-AAG (0.1, 0.5, 1 μM). The black wedges indicate that 17-AAG was added at the start of the 48 h incubation, whereas the gray wedges indicate that 17-AAG was added after 24 h. The relative intensity (*Rel. Int.*) was determined using densitometry and compares the treated cells with the control cells. Gels are representative of at least two independent experiments.

marker of UPR activity, levels of phosphorylated eIF2 α were assessed via immunoblot analysis. Increasing concentrations of 17-AAG resulted in a decrease in phosphorylated eIF2 α levels either alone or in combination with lovastatin (Figure 4c). This effect was most evident in cells treated concurrently with the two agents as compared with those pre-treated with lovastatin and was consistent across the tested cell lines. Treatment with BFA also induced an increase in phosphorylated eIF2 α levels in RPMI-8226, U266 and ALMC-2 cells, which was prevented by co-incubation with 17-AAG (data not shown). Finally, RT-PCR for XBP-1²⁷ demonstrated that 17-AAG prevents lovastatin or BFA-induced XBP-1 mRNA splicing (Supplementary Figure 11).

4-phenylbutyric acid (PBA) is generally considered to be a chemical chaperone that downregulates components of the UPR in other cell types.^{30,31} It was hypothesized that 4-PBA, by serving as a chaperone alternative, could abrogate the effects of IBP inhibitor-mediated disruption of MP trafficking. 4-PBA alone had

modest effects on intracellular lambda light chain levels in RPMI-8226 and ALMC-2 cells (Figure 5a). The addition of 4-PBA to lovastatin partially abrogated the induced increase in intracellular light chain levels. In ALMC-2 cells, the most pronounced effect was the prevention of the 17-AAG-induced increase in intracellular light chain levels. The effects of 4-PBA on lovastatin- and/or 17-AAG-induced changes in UPR component expression were also assessed (Figure 5b). In the RPMI-8226 cells, treatment with 4-PBA alone reduced GADD153 expression and significantly decreased the expression of all UPR markers in cells treated with both lovastatin and 4-PBA compared with lovastatin alone. Similar effects were observed when immunoblot analysis was performed (Supplementary Figure 12). In the U266 cells, 4-PBA increased the expression of ATF6 and partially blocked the lovastatin-induced upregulation of PERK and IRE1. Interestingly, 4-PBA significantly decreased the expression of all tested UPR components in the ALMC-2 cell line and abrogated the effects of lovastatin.

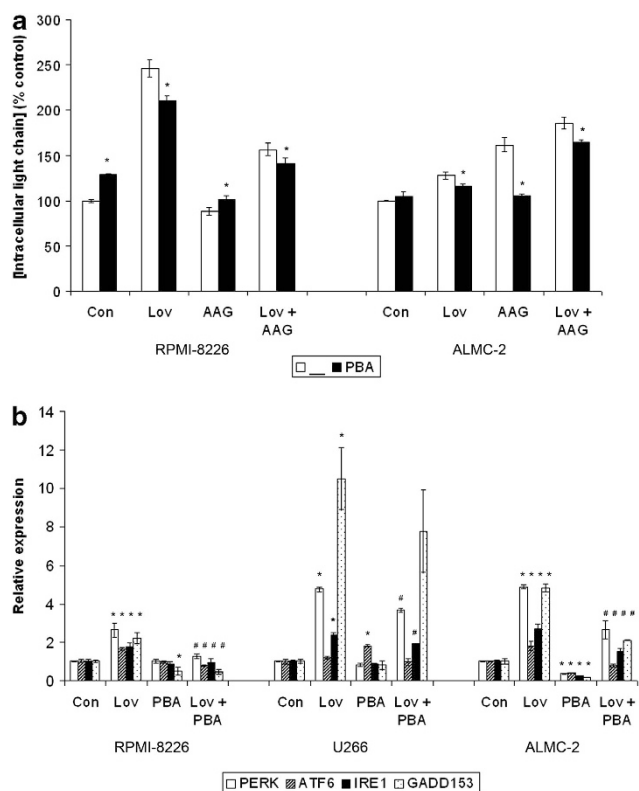


Figure 5. The chemical chaperone 4-PBA augments the effects of HSP90 and IBP inhibition on monoclonal protein trafficking and induction of the UPR. **(a)** RPMI-8226 and ALMC-2 cells were treated with 10 μ M lovastatin (*Lov*), 0.5 μ M 17-AAG (*AAG*) and/or 0.5 mM 4-PBA (*PBA*) for 48 h. Intracellular lambda light chain levels were measured via ELISA. Data are expressed as percentage of control untreated cells (mean \pm s.d., $n = 3$) and are representative of three independent experiments. The * denotes $P < 0.05$ per unpaired two-tailed *t*-test and compares treatments with and without 4-PBA. **(b)** Real-time PCR was performed using primers for PERK, ATF6, IRE1 and GADD153 following incubation of RPMI-8226, U266 or ALMC-2 cells with 10 μ M lovastatin (*Lov*) and/or 0.5 mM 4-PBA (*PBA*) for 48 h. Data were normalized to β -actin levels and are expressed as relative to control untreated cells (mean \pm s.d., $n = 3$). Data are representative of two independent experiments. The * denotes $P < 0.05$ per unpaired two-tailed *t*-test and compares treated cells with control cells. The # denotes $P < 0.05$ for the combination of lovastatin and 4-PBA compared with lovastatin alone.

Addition of 4-PBA reduced lovastatin-induced cytotoxicity by approximately 5% (Supplementary Figure 13). Addition of 4-PBA to 17-AAG did not significantly alter expression patterns compared with 17-AAG alone (data not shown).

HSP90 inhibitors are known to have effects on the expression of other chaperones, but the effects of mevalonate depletion and disruption of MP trafficking on chaperone expression have yet to be explored. Studies were performed with 17-AAG and lovastatin investigating their effects on the expression of key chaperones. GRP78 (immunoglobulin heavy chain binding protein (BiP)) and GRP94 are the ER chaperones that are generally considered to be the most important for mediating the folding of newly synthesized immunoglobulin.³² As expected, 17-AAG markedly upregulated the expression of HSP70, and, to a lesser extent, the related family member HSC70, in RPMI-8226, U266 and H929 cells (Figure 6a). Interestingly, a much more modest effect on HSP70 expression was observed in ALMC-2 cells, and, in contrast to the other two cell lines, a marked decrease in HSC70 expression was noted. A marked decrease in both GRP78 and GRP94 expressions

was observed in the RPMI-8226 and U266 cell lines following treatment with 17-AAG. Lovastatin consistently upregulated GRP78 expression, albeit by 1.5- to 2.5-fold in all tested cell lines and had variable effects on HSP70/HSC70/GRP94 expression. Interestingly, the combination of lovastatin and 17-AAG yielded differential effects in the tested cell lines. In the RPMI-8226 and H929 cells, there was a further increase in HSP70 expression, while the combination resulted in a decrease in HSP70 expression compared with 17-AAG alone in the U266 cells and ALMC-2 cells. The 17-AAG-induced downregulation of GRP78 and GRP94 was abrogated by lovastatin.

The effects of 17-AAG and BFA on chaperone expression were also examined. BFA induces the upregulation of HSP70, GRP78 and GRP94 but not HSC70 in RPMI-8226 and U266 cells (Figure 6b). The combination of the two agents resulted in enhanced upregulation of HSP70 while suppressing the 17-AAG-induced upregulation of HSC70 and the 17-AAG-induced downregulation of GRP78 and GRP94. To determine whether the chemical chaperone 4-PBA influences the expression of these chaperones, cells were treated in the presence or absence of 4-PBA for 48 h. As shown in Figure 6c, 4-PBA did not induce changes in HSP70, HSC70, GRP78 or GRP94 expression in either RPMI-8226 or U266 cells, with the exception of an $\sim 20\%$ decrease in GRP78 expression in RPMI-8226 cells. In contrast, 4-PBA significantly decreased the expression of HSP70, GRP78 and GRP94 in ALMC-2 cells.

DISCUSSION

Chaperones and the unfolded protein response pathway have key roles in the homeostatic regulation of antibody production in plasma cells. Agents that target these processes have important therapeutic implications for the management of multiple myeloma. In the studies presented here, we have demonstrated that the strategy of combining an HSP90 inhibitor with agents that disrupt MP trafficking results in enhanced apoptosis of myeloma cells characterized by complex effects on the UPR and relevant chaperone proteins.

In our studies we demonstrate that the combination of lovastatin and 17-AAG results in enhanced cell death as determined by MTT assays, Annexin V-PI studies, and analysis of PARP, calnexin, caspase-3, caspase-8 and caspase-9 cleavage (Table 1, Supplementary Figure 1, Figure 1). These effects are both concentration- and time-dependent with respect to 17-AAG. It was hypothesized that, if the predominant mechanism of action underlying these effects was via ER stress-induced apoptosis, then caspase-2 or caspase-4 specific inhibitors would prevent the induction of apoptosis. However, only cleavage of calnexin was completely prevented by these caspase inhibitors, and induction of the UPR was abrogated by 17-AAG. Thus, while ER stress-mediated pathways are important for this drug interaction, there is also clear evidence that the classic intrinsic (caspases 9 and 3) and extrinsic (caspases 8 and 3) apoptotic pathways are involved as well. Of note, inhibition of HSP72, an HSP70 family member, has been shown to enhance HSP90 inhibitor-induced apoptosis in myeloma cells primarily through the intrinsic pathway.³³ Thus, our findings from the studies assessing chaperones (Figure 6) further emphasize the connection between induced changes in chaperone expression and apoptosis in myeloma cells.

Our studies revealed that 17-AAG partially abrogated the intracellular accumulation of MP induced by agents that disrupt protein trafficking in myeloma cells (Figure 2, Supplementary Figure 4). Possible mechanisms for these intriguing results include increased secretion, decreased protein synthesis or increased degradation as a result of decreased chaperone activity. 17-AAG did not increase lambda light chain secretion (Supplementary Figure 5) nor did it alter lambda light chain mRNA levels (Supplementary Figure 6). The observed decrease in

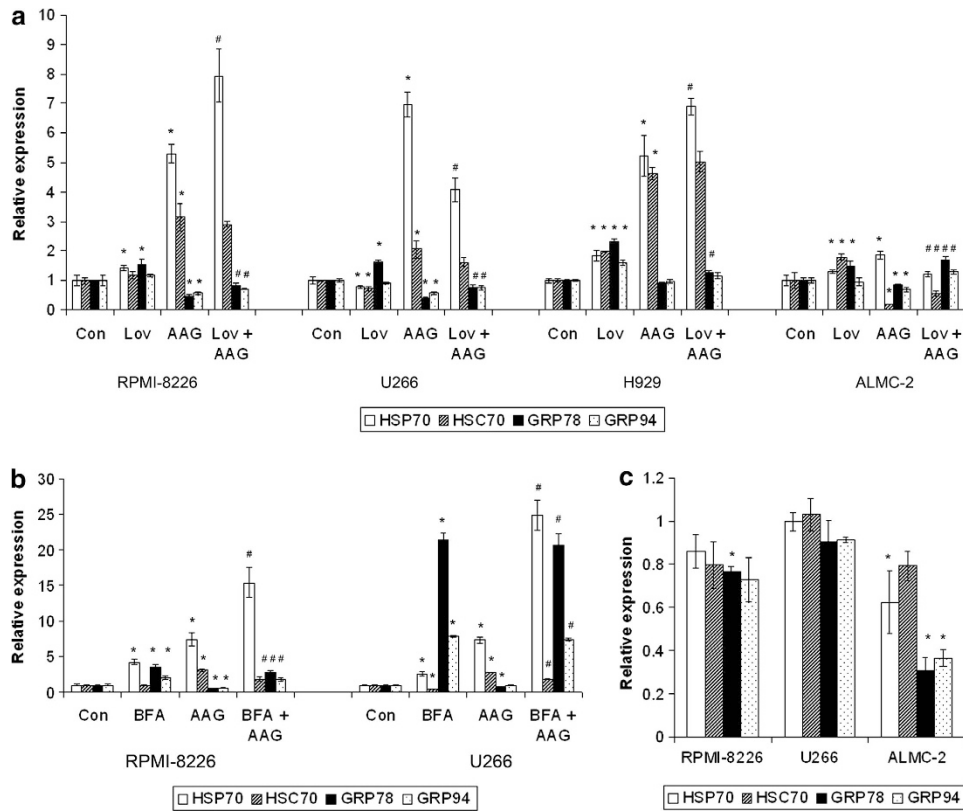


Figure 6. Effects of HSP90 and IBP inhibition on the expression of key chaperones. Real-time PCR studies were performed using primers for HSP70, HSC70, GRP78 and GRP94. Data were normalized to β -actin levels and are expressed as relative to control untreated cells (mean \pm s.d., $n = 3$). Data are representative of two independent experiments. **(a)** RPMI-8226, U266, H929 and ALMC-2 cells were incubated for 48 h in the presence or absence of lovastatin (Lov) and/or 17-AAG (AAG). For the RPMI-8226, U266 and ALMC-2 cells, 10 μ M lovastatin and 0.5 μ M 17-AAG were used, whereas for the H929 cells, 2.5 μ M lovastatin and 0.25 μ M 17-AAG were used. The * denotes $P < 0.05$ per unpaired two-tailed t -test and compares treated cells with control cells. The # denotes $P < 0.05$ for the combination of lovastatin and 17-AAG compared with 17-AAG alone. **(b)** RPMI-8226 and U266 cells were treated with 0.5 μ M brefeldin A (BFA) and/or 0.5 μ M 17-AAG (AAG) for 24 h. The * denotes $P < 0.05$ per unpaired two-tailed t -test and compares treated cells with control cells. The # denotes $P < 0.05$ for the combination of brefeldin A and 17-AAG compared with 17-AAG alone. **(c)** RPMI-8226, U266 and ALMC-2 cells were incubated in the presence of 0.5 mM 4-PBA for 48 h. The * denotes $P < 0.05$ per unpaired two-tailed t -test and compares treated cells with control cells.

phosphorylated eIF2 α levels following 17-AAG treatment (Figure 4c) argues against a global decrease in protein synthesis. Supporting the hypothesis that the mechanism involves increased protein degradation as a result of decreased chaperone activity are the observations that 17-AAG induces a marked down-regulation of both GRP78 and GRP94, the key chaperones involved in immunoglobulin folding (Figure 6) and that the addition of the proteasome inhibitor bortezomib to either lovastatin or lovastatin/17-AAG resulted in an increase in intracellular protein levels (Figure 2f). Recent studies have investigated the relationship between the proteasome pathway and autophagy in myeloma.³⁴ Whether MP, particularly aggregated protein located outside of the ER such as what occurs following lovastatin treatment, can be degraded via autophagy remains to be determined.

Many of the UPR genes share common promoter elements, including the ER stress element (ERSE) and the UPR element (UPRE). The studies by Takayanagi *et al.*³⁵ have revealed a complex regulatory network containing feedback loops, which governs the response of UPR genes to ER stress. Agents that induce ER stress, such as thapsigargin and tunicamycin, transcriptionally upregulate a variety of UPR genes, including XBP1, CHOP, PERK, IRE1, ATF4, but not ATF6 in HeLa cells.³⁵ Our studies have revealed a similar pattern of transcriptional regulation in response to agents that disrupt Rab geranylgeranylation (Figure 4a, Supplementary Figure 9), thus demonstrating that disrupting protein trafficking

is an effective mechanism to induce ER stress in malignant plasma cells.

There have been conflicting reports regarding the effects of HSP90 inhibitors on the UPR in myeloma cells. Davenport *et al.*²⁸ reported that 17-AAG activated the key mediators of the UPR within 2–4 h in U266 cells. The differences between their observed results and our results with the U266 line (Figure 4a) may be due to different time points (<4 vs >24 h) and concentration of 17-AAG (5 vs 0.5 μ M). In contrast, IPI-504, a pro-drug of 17-AAG, decreased UPR and ER stress element activation in U266 and MM.1 cells.³⁶ Treatment of MM.1 cells with IPI-504 for 16 h resulted in decreased phosphorylated eIF2 α levels. In those studies, cells were stimulated with tunicamycin for 15 min before lysis, thus demonstrating a reduced ability to phosphorylate eIF2 α in the presence of ER stress. Our studies demonstrate that treatment with an HSP90 inhibitor results in a concentration-dependent decrease in steady-state levels of phosphorylated eIF2 α (Figure 4c) in all tested cell lines at both 24 and 48 h. This effect was diminished in the presence of lovastatin. Despite similar effects on phospho-eIF2 α levels across the cell lines, examination of the changes in expression of key UPR components revealed cell line-specific patterns, highlighting the importance of understanding how the regulation of the different UPR modulators and resulting response to therapeutic agents varies among myeloma patients.

The activity of 4-PBA in myeloma or amyloid light chain-producing cells has not previously been investigated. 4-PBA

modulates the UPR pathway and reduces ER stress in a variety of cell types. That this agent can rescue cells from mutated proteins, such as CTRF, ATP7B, myocilin, low-density lipoprotein receptor and nephrin,^{37–41} supports the hypothesis that the effects on ER stress and the UPR are secondary to its ability to act as a chemical chaperone, preventing misfolded protein aggregation and restoring trafficking. Our studies are the first to demonstrate that 4-PBA significantly downregulates the expression of UPR components and key chaperones in AL amyloid cells (Figures 5b and 6c). Furthermore, the lovastatin-induced upregulation of UPR components was blocked by co-incubation with 4-PBA. The effects of 4-PBA alone in the myeloma cell lines were less notable; however, 4-PBA did abrogate the effects of lovastatin. The results from the ELISA studies suggest that the decreased UPR activation is not simply a consequence of reduced intracellular MP levels as 4-PBA reduced levels by less than 30% (Figure 5a). Instead, the activity of 4-PBA may be more due to the amelioration of protein misfolding and aggregation than due to changes in absolute protein levels, as misfolded proteins are a potent trigger for UPR activation. From a therapeutic perspective, 4-PBA might provide a means to protect other cell types from amyloid deposition while sensitizing the AL amyloid-producing plasma cell to agents that induce cell death via non-ER stress mediated mechanisms.

In conclusion, these studies reveal that the strategy of simultaneously disrupting MP trafficking and chaperone activity results in a complex modulation of ER stress, UPR and cell death pathways. The observed differences among the myeloma cell lines highlight the importance of exploring the effects of these agents in primary samples, with particular emphasis on different cytogenetic subtypes as well as production/secretion of intact vs light chain-only MP. In these studies, lovastatin was used as a surrogate for a specific GGTase II inhibitor, given the current dearth of potent and selective GGTase II inhibitors. We have used 17-AAG as a representative HSP90 inhibitor, but it is recognized that second or third generation HSP90 inhibitors may ultimately have more clinical potential. These data support the further development of Rab-targeted agents in myeloma as well as pre-clinical and clinical evaluation in combination with other therapeutic agents. The increasing clinical exploration of agents that induce ER stress and apoptosis in myeloma cells, such as proteasome or NEDDylation inhibitors, HSP90 inhibitors and histone deacetylase inhibitors, underscores the importance of furthering our understanding of how these pathways may be manipulated to achieve maximal cytotoxic effects in malignant plasma cells. Furthermore, our work indicates that there are key differences in how amyloidogenic- and non-amyloidogenic-MP-producing cells respond to agents that alter MP trafficking and chaperone activity, suggesting that distinct therapeutic strategies can be devised for these two related, but disparate, plasma cell dyscrasias.

CONFLICT OF INTEREST

The authors declare no conflict of interest.

ACKNOWLEDGEMENTS

We thank The University of Iowa Flow Cytometry Facility and the University of Iowa Central Microscopy Research Facility. This project was supported by the PhRMA Foundation (S.A. Holstein), the Roy J. Carver Charitable Trust (S.A. Holstein), the American Society of Hematology (S.A. Holstein), the NCI Iowa/Mayo Lymphoma Specialized Programs of Research Excellence Career Development Program (S.A. Holstein) and the NIH (R01 CA172070) (S.A. Holstein).

REFERENCES

- 1 Sankhala KK, Mita MM, Mita AC, Takimoto CH. Heat shock proteins: a potential anticancer target. *Curr Drug Targets* 2011; **12**: 2001–2008.
- 2 Mitsiades CS, Mitsiades NS, McMullan CJ, Poulaki V, Kung AL, Davies FE *et al*. Antimyeloma activity of heat shock protein-90 inhibition. *Blood* 2006; **107**: 1092–1100.
- 3 Stuhmer T, Zollinger A, Siegmund D, Chatterjee M, Grella E, Knop S *et al*. Signalling profile and antitumour activity of the novel Hsp90 inhibitor NVP-AUY922 in multiple myeloma. *Leukemia* 2008; **22**: 1604–1612.
- 4 Duus J, Bahar HI, Venkataraman G, Ozpuyan F, Izban KF, Al-Masri H *et al*. Analysis of expression of heat shock protein-90 (HSP90) and the effects of HSP90 inhibitor (17-AAG) in multiple myeloma. *Leukemia Lymphoma* 2006; **47**: 1369–1378.
- 5 Ishii T, Seike T, Nakashima T, Juliger S, Maharaj L, Soga S *et al*. Anti-tumor activity against multiple myeloma by combination of KW-2478, an Hsp90 inhibitor, with bortezomib. *Blood Cancer J* 2012; **2**: e68.
- 6 Richardson PG, Chanan-Khan AA, Lonial S, Krishnan AY, Carroll MP, Alsina M *et al*. Tanespimycin and bortezomib combination treatment in patients with relapsed or relapsed and refractory multiple myeloma: results of a phase 1/2 study. *Br J Haematol* 2011; **153**: 729–740.
- 7 Brewer JW, Hendershot LM. Building an antibody factory: a job for the unfolded protein response. *Nat Immunol* 2005; **6**: 23–29.
- 8 Malhotra JD, Kaufman RJ. The endoplasmic reticulum and the unfolded protein response. *Semin Cell Dev Biol* 2007; **18**: 716–731.
- 9 Yoshida H, Okada T, Haze K, Yanagi H, Yura T, Negishi M *et al*. ATF6 activated by proteolysis binds in the presence of NF- κ B (CBF) directly to the cis-acting element responsible for the mammalian unfolded protein response. *Mol Cell Biol* 2000; **20**: 6755–6767.
- 10 Harding HP, Zhang Y, Ron D. Protein translation and folding are coupled by an endoplasmic-reticulum-resident kinase. *Nature* 1999; **397**: 271–274.
- 11 Breckenridge DG, Germain M, Mathai JP, Nguyen M, Shore GC. Regulation of apoptosis by endoplasmic reticulum pathways. *Oncogene* 2003; **22**: 8608–8618.
- 12 Ma Y, Brewer JW, Diehl JA, Hendershot LM. Two distinct stress signaling pathways converge upon the CHOP promoter during the mammalian unfolded protein response. *J Mol Biol* 2002; **318**: 1351–1365.
- 13 Ron D, Habener JF. CHOP, a novel developmentally regulated nuclear protein that dimerizes with transcription factors C/EBP and LAP and functions as a dominant-negative inhibitor of gene transcription. *Genes Dev* 1992; **6**: 439–453.
- 14 Nakagawa T, Zhu H, Morishima N, Li E, Xu J, Yankner BA *et al*. Caspase-12 mediates endoplasmic reticulum-specific apoptosis and cytotoxicity by amyloid-beta. *Nature* 2000; **403**: 98–103.
- 15 Hitomi J, Katayama T, Eguchi Y, Kudo T, Taniguchi M, Koyama Y *et al*. Involvement of caspase-4 in endoplasmic reticulum stress-induced apoptosis and Abeta-induced cell death. *J Cell Biol* 2004; **165**: 347–356.
- 16 Rao RV, Ellerby HM, Bredesen DE. Coupling endoplasmic reticulum stress to the cell death program. *Cell Death Differ* 2004; **11**: 372–380.
- 17 Gu H, Chen X, Gao G, Dong H. Caspase-2 functions upstream of mitochondria in endoplasmic reticulum stress-induced apoptosis by bortezomib in human myeloma cells. *Mol Cancer Ther* 2008; **7**: 2298–2307.
- 18 Obeng EA, Carlson LM, Gutman DM, Harrington Jr WJ, Lee KP, Boise LH. Proteasome inhibitors induce a terminal unfolded protein response in multiple myeloma cells. *Blood* 2006; **107**: 4907–4916.
- 19 Holstein SA, Hohl RJ. Isoprenoid biosynthetic pathway inhibition disrupts monoclonal protein secretion and induces the unfolded protein response pathway in multiple myeloma cells. *Leuk Res* 2011; **35**: 551–559.
- 20 Shull LW, Wiemer AJ, Hohl RJ, Wiemer DF. Synthesis and biological activity of isoprenoid bisphosphonates. *Bioorg Med Chem* 2006; **14**: 4130–4136.
- 21 Coxon FP, Helfrich MH, Larjani B, Muzylak M, Dunford JE, Marshall D *et al*. Identification of a novel phosphonocarboxylate inhibitor of Rab geranylgeranyl transferase that specifically prevents Rab prenylation in osteoclasts and macrophages. *J Biol Chem* 2001; **276**: 48213–48222.
- 22 Arendt BK, Ramirez-Alvarado M, Sikkink LA, Keats JJ, Ahmann GJ, Dispenzieri A *et al*. Biologic and genetic characterization of the novel amyloidogenic lambda light chain-secreting human cell lines, ALMC-1 and ALMC-2. *Blood* 2008; **112**: 1931–1941.
- 23 Holstein SA, Hohl RJ. Interaction of cytosine arabinoside and lovastatin in human leukemia cells. *Leuk Res* 2001; **25**: 651–660.
- 24 Chou TC, Talalay P. Quantitative analysis of dose-effect relationships: the combined effects of multiple drugs or enzyme inhibitors. *Adv Enzyme Regul* 1984; **22**: 27–55.
- 25 Morishima N, Nakanishi K, Takenouchi H, Shibata T, Yasuhiko Y. An endoplasmic reticulum stress-specific caspase cascade in apoptosis. Cytochrome c-independent activation of caspase-9 by caspase-12. *J Biol Chem* 2002; **277**: 34287–34294.
- 26 Nakagawa T, Zhu H, Morishima N, Li E, Xu J, Yankner BA *et al*. Caspase-12 mediates endoplasmic-reticulum-specific apoptosis and cytotoxicity by amyloid-beta. *Nature* 2000; **403**: 98–103.

- 27 Obeng EA, Boise LH. Caspase-12 and caspase-4 are not required for caspase-dependent endoplasmic reticulum stress-induced apoptosis. *J Biol Chem* 2005; **280**: 29578–29587.
- 28 Davenport EL, Moore HE, Dunlop AS, Sharp SY, Workman P, Morgan GJ *et al*. Heat shock protein inhibition is associated with activation of the unfolded protein response pathway in myeloma plasma cells. *Blood* 2007; **110**: 2641–2649.
- 29 Misumi Y, Miki K, Takatsuki A, Tamura G, Ikehara Y. Novel blockade by brefeldin A of intracellular transport of secretory proteins in cultured rat hepatocytes. *J Biol Chem* 1986; **261**: 11398–11403.
- 30 de Almeida SF, Picarote G, Fleming JV, Carmo-Fonseca M, Azevedo JE, de Sousa M. Chemical chaperones reduce endoplasmic reticulum stress and prevent mutant HFE aggregate formation. *J Biol Chem* 2007; **282**: 27905–27912.
- 31 Kubota K, Niinuma Y, Kaneko M, Okuma Y, Sugai M, Omura T *et al*. Suppressive effects of 4-phenylbutyrate on the aggregation of Pael receptors and endoplasmic reticulum stress. *J Neurochem* 2006; **97**: 1259–1268.
- 32 Melnick J, Dul JL, Argon Y. Sequential interaction of the chaperones BiP and GRP94 with immunoglobulin chains in the endoplasmic reticulum. *Nature* 1994; **370**: 373–375.
- 33 Davenport EL, Zeisig A, Aronson LI, Moore HE, Hockley S, Gonzalez D *et al*. Targeting heat shock protein 72 enhances Hsp90 inhibitor-induced apoptosis in myeloma. *Leukemia* 2010; **24**: 1804–1807.
- 34 Aronson LI, Davenport EL, Mirabella F, Morgan GJ, Davies FE. Understanding the interplay between the proteasome pathway and autophagy in response to dual PI3K/mTOR inhibition in myeloma cells is essential for their effective clinical application. *Leukemia* 2013; e-pub ahead of print 14 May 2013; doi:10.1038/leu.2013.150.
- 35 Takayanagi S, Fukuda R, Takeuchi Y, Tsukada S, Yoshida K. Gene regulatory network of unfolded protein response genes in endoplasmic reticulum stress. *Cell Stress Chaperones* 2012; **18**: 11–23.
- 36 Patterson J, Palombella VJ, Fritz C, Normant E. IPI-504, a novel and soluble HSP-90 inhibitor, blocks the unfolded protein response in multiple myeloma cells. *Cancer Chemother Pharmacol* 2008; **61**: 923–932.
- 37 Yam GH, Gaplovska-Kysela K, Zuber C, Roth J. Sodium 4-phenylbutyrate acts as a chemical chaperone on misfolded myocilin to rescue cells from endoplasmic reticulum stress and apoptosis. *Invest Ophthalmol Vis Sci* 2007; **48**: 1683–1690.
- 38 Tveten K, Holla OL, Ranheim T, Berge KE, Leren TP, Kulseth MA. 4-Phenylbutyrate restores the functionality of a misfolded mutant low-density lipoprotein receptor. *FEBS J* 2007; **274**: 1881–1893.
- 39 van den Berghe PV, Stapelbroek JM, Krieger E, de Bie P, van de Graaf SF, de Groot RE *et al*. Reduced expression of ATP7B affected by Wilson disease-causing mutations is rescued by pharmacological folding chaperones 4-phenylbutyrate and curcumin. *Hepatology* 2009; **50**: 1783–1795.
- 40 Liu XL, Done SC, Yan K, Kilpelainen P, Pikkariainen T, Tryggvason K. Defective trafficking of nephrin missense mutants rescued by a chemical chaperone. *J Am Soc Nephrol* 2004; **15**: 1731–1738.
- 41 Zeitlin PL, Diener-West M, Rubenstein RC, Boyle MP, Lee CK, Brass-Ernst L. Evidence of CFTR function in cystic fibrosis after systemic administration of 4-phenylbutyrate. *Mol Ther* 2002; **6**: 119–126.



This work is licensed under a Creative Commons Attribution-NonCommercial-NoDerivs 3.0 Unported License. To view a copy of this license, visit <http://creativecommons.org/licenses/by-nc-nd/3.0/>

Supplementary Information accompanies this paper on Blood Cancer Journal website (<http://www.nature.com/bcj>)